

Enhancing virtual reality with high-resolution light field liquid crystal display technology

Yung-Hsun Wu¹,^{a,*} Chuan-Chung Chang,^b Yu-Shih Tsou,^a Yi-Chien Lo,^b
Chia-Hao Tsai,^a Chih-hung Lu,^b Chiu-Lien Yang,^a and Fu-Ming Chuang^b

^aInnolux Corporation, Miaoli, Taiwan

^bCoretronic Corporation, Hsinchu, Taiwan

ABSTRACT. An improved light field VR display is introduced, featuring an ultra-high-pixel density liquid crystal display with a resolution of 3.1 in. and 1411 PPI. By utilizing a 3K3K resolution display panel, this optimized display enhances the field of view and provides a more immersive experience. Furthermore, it incorporates advanced functions, such as vision correction (without the need for glasses), reduced vergence-accommodation conflict, and an enlarged eye box with eye tracking technology.

© The Authors. Published by SPIE under a Creative Commons Attribution 4.0 International License. Distribution or reproduction of this work in whole or in part requires full attribution of the original publication, including its DOI. [DOI: [10.1117/1.JOM.3.4.041202](https://doi.org/10.1117/1.JOM.3.4.041202)]

Keywords: light field; display; VR; liquid crystal display; vergence-accommodation conflict free; vision correction; high resolution; high PPI; wide field of view

Paper 23008SS received Jun. 1, 2023; revised Jul. 29, 2023; accepted Jul. 31, 2023; published Sep. 13, 2023.

1 Introduction

Near-eye displays are being considered as the future of portable devices, providing virtual reality experiences for individuals. The main goals in developing these displays are to create immersive experiences and ensure visual comfort. In virtual reality, a larger field of view (FOV) enhances immersion, but it is also important to reduce the vergence-accommodation conflict (VAC) for comfortable vision.¹⁻⁴ Researchers have explored various spatial and time multiplexed approaches to address these challenges.⁵⁻¹⁰ Light field (LF) displays play a crucial role in improving near-eye displays. However, previous LF displays were limited by their small size and low resolution, resulting in narrow viewing angles and screen window effects due to low resolution. We have successfully addressed these limitations and achieved more realistic LF images by utilizing a 3.1-in. 3K3K display.¹¹ However, the development of large-scale, high-resolution virtual reality (VR) liquid crystal display (LCD) displays poses challenges in terms of process and material constraints that need to be overcome. This paper discusses the importance of increasing the aperture ratio and improving contrast ratio (CR) through specialized driving methods and pixel designs. Additionally, we explore the use of LF technology for vision correction and expanding the eyebox to enhance the VR visual experience. It is worth noting that this LF technology also has the potential to correct vision, further improving visual comfort and user experience in near-eye displays.

2 Architecture and Design

2.1 Optics of Light Field VR

In Fig. 1, we observe the generation of an elemental image (EI) array through a lens array using spatial multiplexed LF optics. Unlike non-LF optics, LF technology enables the provision of

*Address all correspondence to Yung-Hsun Wu, yhwu0922@gmail.com

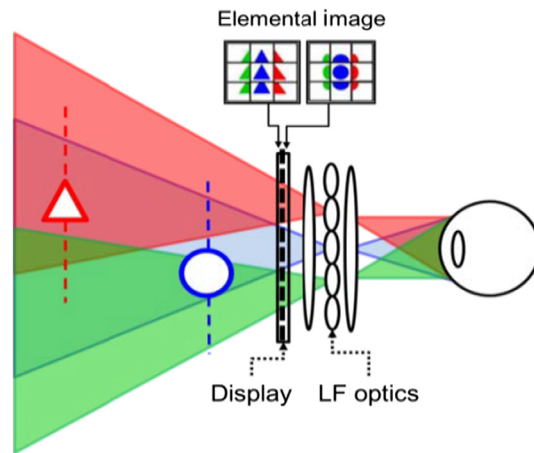


Fig. 1 Multi-depth image via spatial multiplexed LF optics with EI.

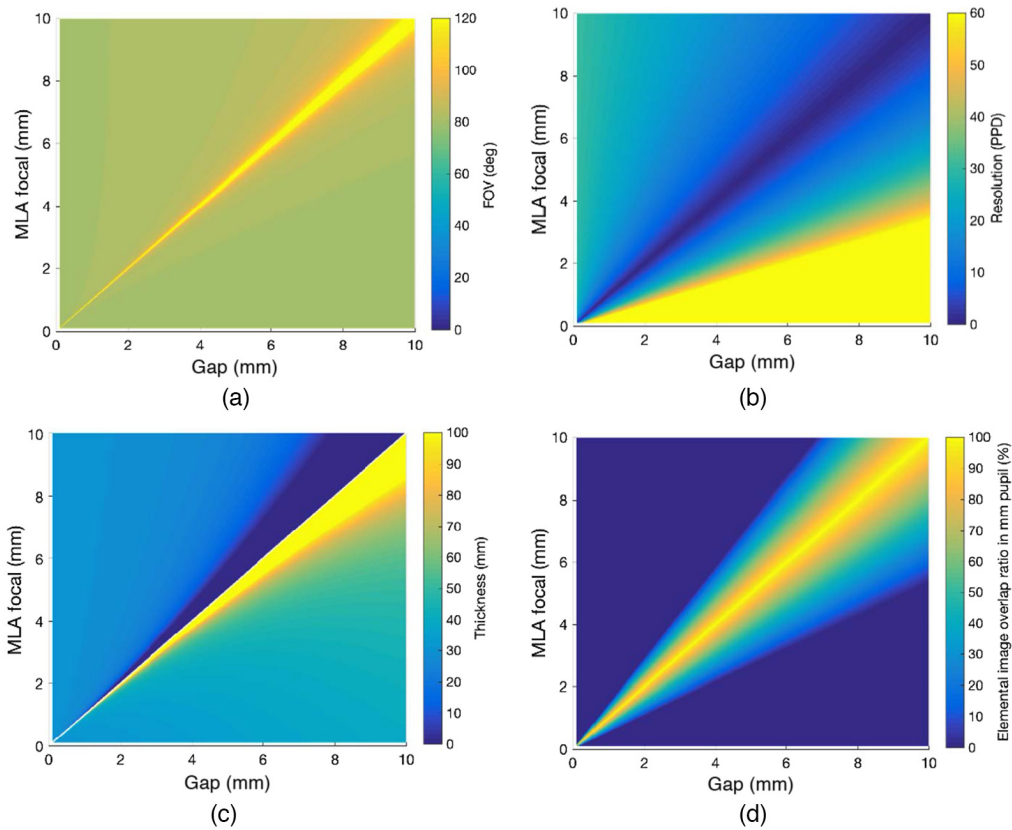


Fig. 2 First order design parameters and boundary conditions: (a) FOV, (b) resolution, (c) total thickness, and (d) overlapping ratio with focal length of lens array and object distance (gap between lens array and panel).

volumetric virtual images that accurately simulate the correct disparity of each EI, allowing viewers to experience correct eye accommodation. This eliminates the need for VAC for observers. By carefully considering first-order design parameters and boundary conditions, such as FOV, resolution, total thickness, and overlapping ratio with focal length of microlens array (MLA), as depicted in Fig. 2, we can achieve optimal results.

In this paper, we focus on a newly developed LCD by INNOLUX, boasting a resolution of 3240×2880 pixels and a high-pixel density of 1440 PPI (pixels per inch). The effective display area measures $58.32 \times 51.84 \text{ mm}^2$. Considering a monocular viewing scenario, the best FOV

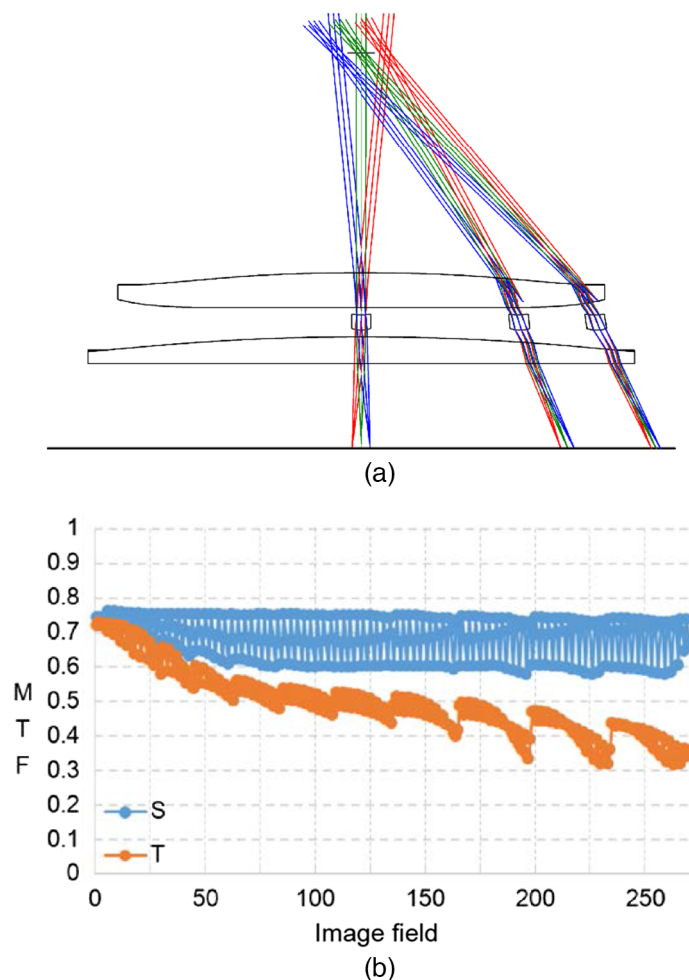


Fig. 3 Designed LF (a) optical layout of designed LF and (b) MTF of designed LF optics.

achieved is $70 \text{ deg} \times 65 \text{ deg}$ with an eye relief of 29 mm and an eye box of 6.4 mm. To further enhance the horizontal FOV in binocular vision, a 15-deg tilt between the panels is incorporated, as illustrated in Fig. 3. This design modification expands the binocular FOV to an impressive $100 \text{ deg} \times 65 \text{ deg}$, with an angular resolution exceeding 15 pixels per degree (PPD).

To ensure high-quality image reproduction, the designed modulation transfer function (MTF) across the entire image field surpasses 30% at the Nyquist frequency of 28 line pairs per millimeter (lp/mm), as demonstrated in Fig. 3. This indicates that the display system is capable of accurately reproducing fine details and maintaining image clarity. Through these advancements, our research contributes to the development of LF display technologies, enabling an immersive visual experience with volumetric virtual images, expanded FOV, and improved image quality.

2.2 High-Resolution VR LCD

2.2.1 Wide field of view

High resolution (large panel size) provides a wide FOV.¹² High resolution also helps to simplify the optical system design of the VR head-mounted display. However, there are more gate lines in a high-resolution panel than in a low-resolution panel. The more gate lines take more scanning time. This will decrease the refresh rate and increase moving picture response time (MPRT).¹³ Thus an optimization between the resolution and MPRT is needed. INNOLUX proposes a 3K3K resolution 1411 PPI display panel, which provides a virtual image with binocular FOV 100 deg in VR optical system and also maintains the 15 PPD image quality, as shown in Fig. 4.



Fig. 4 FOV improvement from 80 deg to 100 deg.

2.2.2 Fast moving picture response

MPRT is a general indicator of the motion quality of a display. Generally speaking, the MPRT of a display panel in VR system should be <1.5 ms, otherwise, users will see the motion blur when an object moves fast in the screen. To achieve such a fast MPRT in a 3K3K high-resolution display panel, we set the refresh rate at 75 Hz with a 10% duty ratio blinking backlight. We also improve the scanning time of 3000 gate lines within 9 ms and LC response time within 3 ms. The measured MPRT is about 1.1 ms as shown in Fig. 5, which provides a high-quality moving picture without motion blur.

2.2.3 Circuit design

When the panel resolution is increased, the loading of the gate driver circuit (GDC) will become heavier, so it is necessary to increase the size of the components to improve the driving capability, resulting in larger left and right borders. When the resolution is increased, the vertical space of GDC of each pixel will become smaller, so the circuit design can only be laid out in the horizontal space, resulting in larger borders on the left and right sides of the panel. Considering the requirement of interpupillary distance, the left and right borders need to be controlled below 2 mm. Therefore, Innolux developed GDC 1-to-4 driver circuit and short-channel component design to reduce borders in the future to meet the needs of products, as shown in Fig. 6.

High-resolution and high-frequency driven pixel charging times are short. Therefore, small signal distortion will affect the ability to charge. When the resolution and driving frequency are increased at the same time, the RC load becomes heavier, and it is difficult to realize high-frequency driving. In order to solve the problem of insufficient charging, we use three-terminal input in the circuit design, strengthen the driving ability, optimize the signal line load, and reduce the signal distortion phenomenon. This enables higher-resolution high-frequency drive, provides faster picture refresh rates, and solves dynamic image smearing issues, as shown in Fig. 7.

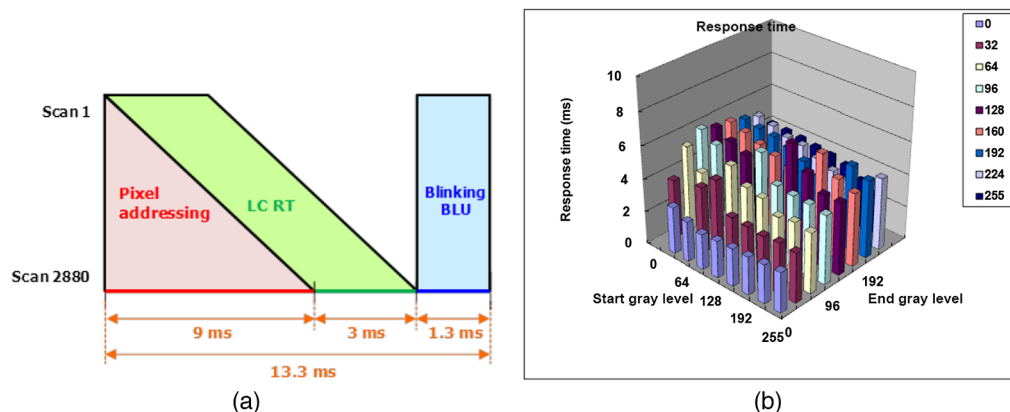


Fig. 5 (a) Addressing timing and (b) LC response time.

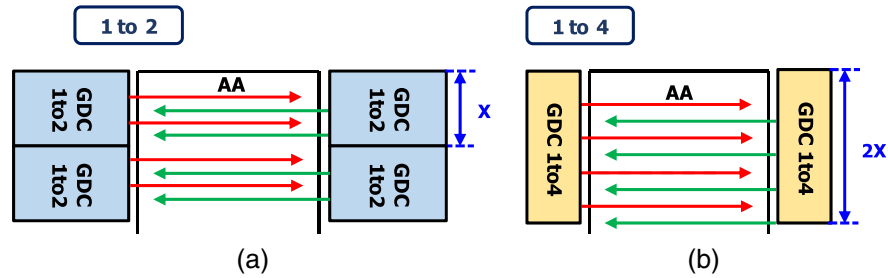


Fig. 6 1:4 GDC: (a) GDC 1-to-2 and (b) GDC 1-to-4.

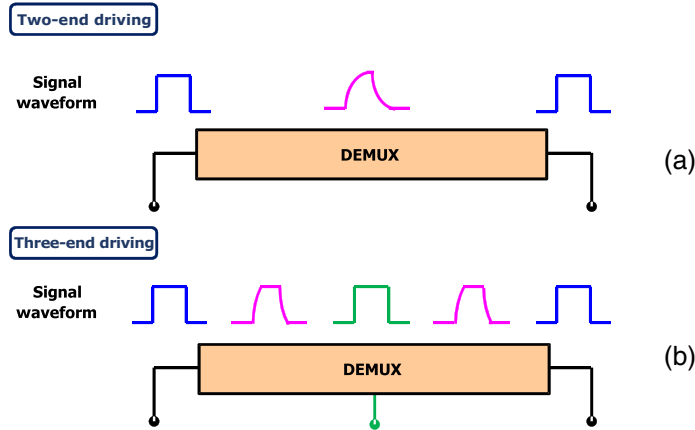


Fig. 7 DEMUX three-end driving: (a) two-terminal input and (b) three-terminal input.

2.2.4 High brightness and contrast ratio

The brightness and CR are also important specifications in a VR display. High brightness and high CR bring the immersion to the users.¹⁴ However, when the pixel becomes such a small size as 1411 PPI, many issues come out because of the low aperture ratio. For example, we have to adopt the metal layer as the black matrix to avoid the BM rounding effect, as we mention in our previous paper.¹⁵ The optical design should be optimized to keep the brightness and CR. In this paper, to increase the aperture ratio, we change the pixel arrangement so that two pixels share the black matrix near the TFT device, as shown in Fig. 8. This arrangement decreases the area of black matrix and increases the aperture ratio.

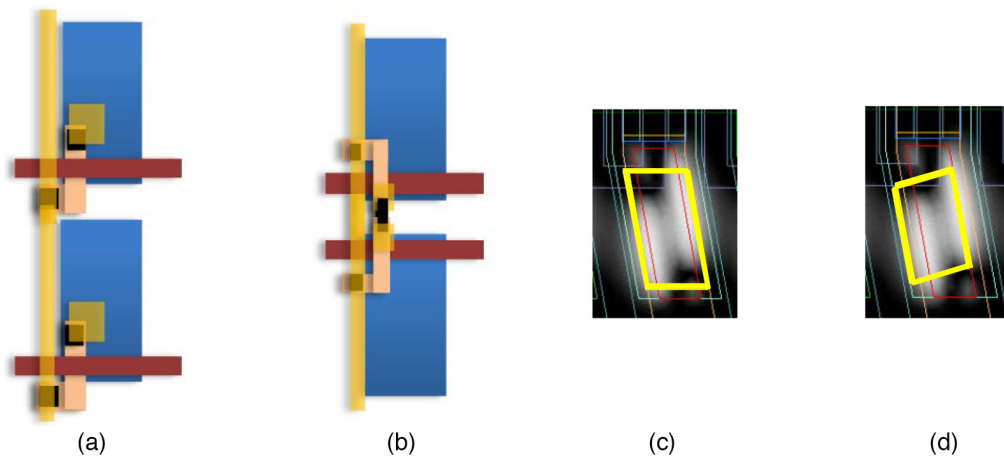


Fig. 8 (a) Traditional pixel arrangement, (b) BM shared pixel arrangement, (c) traditional aperture design, and (d) optimized aperture design.

The LC dark fringe caused by the relief of TFT device is ignorable in a large size pixel. However, it is critical in a small size pixel because the dark fringe results in a low CR. To improve the CR, we optimize the shape of aperture area such that the dark fringe is blocked and the bright fringe is transmitted. As a result, the CR is increased, as shown in Fig. 8.

2.2.5 Higher resolution VR LCD

This paper discusses the utilization of a 3K3K VR LCD for LF display in VR applications. However, recent advancements in display technology have introduced 4k VR LCDs, as highlighted in the 2023 SID conference by both Innolux Corp.¹⁶ and BOE Technology Group.¹⁷ Incorporating this new technological development, along with the LF techniques described in this paper, holds the potential to enhance the resolution of LF displays. Additionally, it enables the expansion of the eyebox, currently at 6.4 mm, surpassing the current limit of 15 PPD, thus further improving the overall visual experience.

2.3 Visual Correction

In order to further simplify computation complexity in LFVR, a ray tracing-based graphic process “corrected eye box mapping” for full visual-corrected function is also included, correction for myopia, hyperopia, and even astigmatism are completed as reported perilously.¹⁸ In order to obtain comprehensive visual-corrected function, spherical power (SPH), cylinder power (CYL), and cylinder axis (AXIS) should all be considered. As shown in Fig. 9, corrected eye box is scaled into different sizes and directions based on the original eye box size. For adjusting the SPH, the corrected eye box size is scaled according to the center, as shown in Fig. 9(a). For adjusting the CYL and AXIS, the corrected eye box size is scaled in the different ratios and rotation angles from the original eye box size in specific axis, as shown in Figs. 9(b) and 9(c). Similarly, in cases of irregular astigmatism, the content will be rearranged based on the corrected eye box size. The simulations conducted in LightTools involve the replication of -4D astigmatism in different rotation angles, as demonstrated in Figs. 10(a) and 10(b). The proposed mapping method is then employed to obtain the corrected results, as illustrated in Fig. 10(c).

The performance of vision correction was also examined using specific prescriptions: (-3 SPH, -1 CYL, and 45 deg AXIS) and ($+2$ SPH, $+2$ CYL, and 45 deg AXIS). To simulate myopia or hyperopia, a prescription lens with the opposite power and angle was placed in front of the camera. The resulting blurred images can be seen in Figs. 11(a) and 12(a) and displays the camera’s focus at 500 mm. The LF images in Figs. 11(b) and 12(b) demonstrate the successful correction of myopia, hyperopia, and even astigmatism.

2.4 Uniformity Improving

In the LF optics, showing in Fig. 13(a), there is a challenge posed by the partial overlap between EIs, which can result in a non-uniform luminance distribution in the final LF image. This often manifests as a noticeable grid or dot array pattern. To address this issue and further enhance the uniformity of the LF image, a compensating luminance distribution is typically employed, often based on a Gaussian model for each EI. This compensation technique aims to reduce the discrepancy between the maximum and minimum luminance values, as depicted in Fig. 13(b).

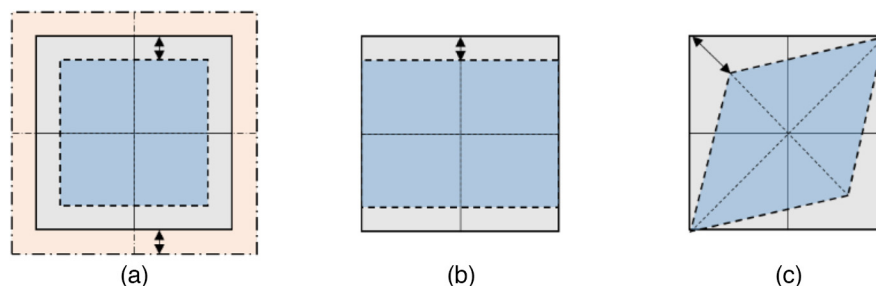


Fig. 9 Corrected eye box mapping for visual correction in (a) SPH and astigmatism of the (b) CYL and (c) AXIS.

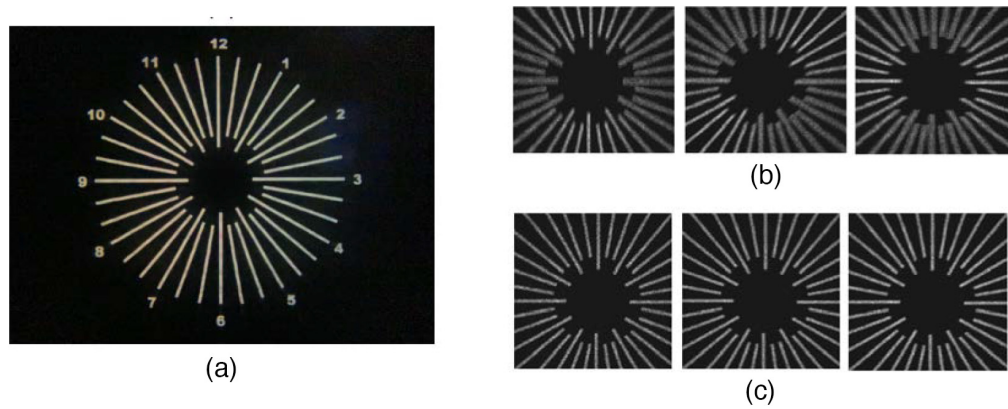


Fig. 10 Proof of concept of LF vision correction (a) reference without astigmatism; (b) astigmatism from left to right: 0 deg, 45 deg, and 90 deg of AST axis; and (c) corrected with proposed eye box mapping method from left to right: 0 deg, 45 deg, and 90 deg.

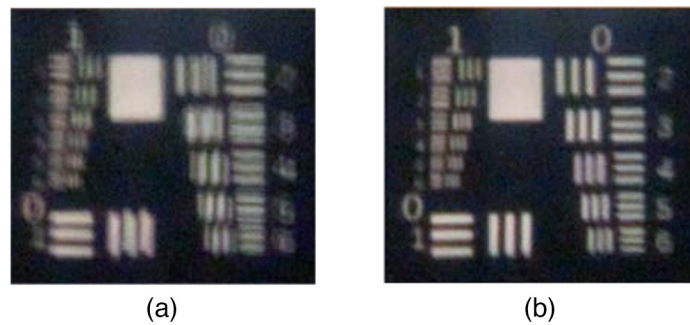


Fig. 11 Captured LF image at 500 mm virtual distance (a) myopia (-3 SPH, -1 CYL, and 45 AXIS) and (b) corrected.

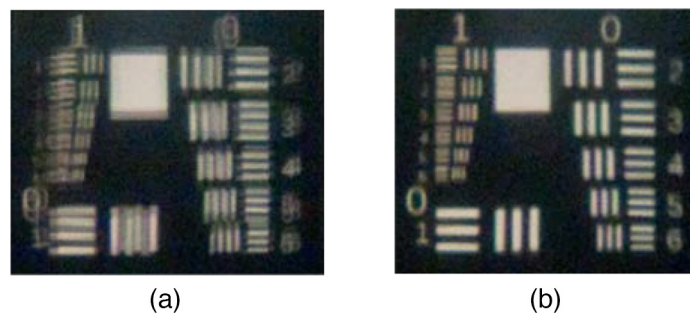


Fig. 12 Captured LF image at 500 mm virtual distance: (a) hyperopia (+2 SPH, +2 CYL, and 45 AXIS) and (b) corrected.

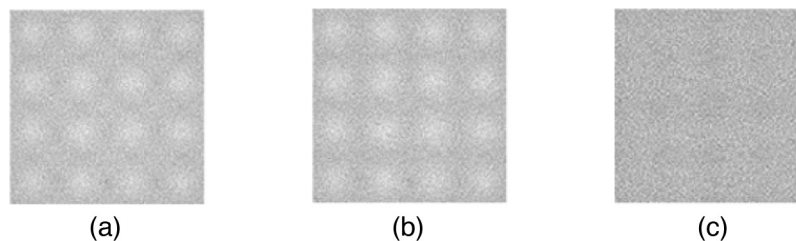


Fig. 13 Brightness uniformity of LF image (a) original without compensation, (b) Gaussian-based compensation, and (c) dynamic modulated compensation.

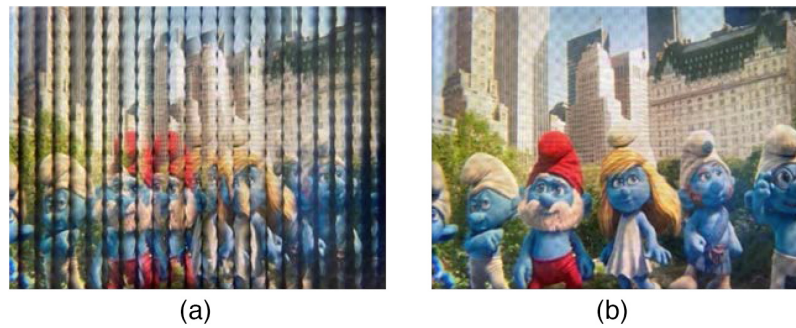


Fig. 14 LF image with 3 mm pupil shift: (a) w/o processing and (b) w/ proposed full digital image calculation.

However, it is important to note that the pupil size of the observer can vary under different ambient brightness conditions. To account for this dynamic change and further improve the luminance uniformity, a modulated compensation approach coupled with an eye tracker is employed. This dynamic modulation compensates for variations in the pupil size and ensures a more consistent luminance distribution across the LF image, as illustrated in Fig. 13(c).

2.5 Eye Box Expansion

In VR products, a larger eye box is a crucial requirement due to the automatic scanning nature of the human eye. However, designing a larger eye box in LF optics involves trade-offs with other first-order parameters. To address this challenge, two approaches have been studied and proposed, both utilizing information from an eye tracker: full digital image calculation and LC-based beam steering.

Figure 14 illustrates the results of the full digital image calculation approach. It is evident that the LF image is free from vignetting and can seamlessly combine even with a 3 mm shift in the eye pupil, as depicted in Fig. 14(b). Moreover, through experimentation, an eye box that is ~ 2 times larger has been successfully achieved.

These findings highlight the effectiveness of the full digital image calculation approach in overcoming the trade-offs associated with designing a larger eye box in LF optics. It demonstrates the potential to enhance the user experience by providing a wider viewing area without compromising image quality or coherence.

3 Prototype and Specification

Specifications of the high-resolution LF VR LCD are summarized in Table 1. The prototype demonstration is also shown in Fig. 15. The LCD panel provides a high-quality 3K3K resolution image with 1411 PPI and 1.1 ms MPRT. The LF VR system provides a 100 deg \times 65 deg binocular FOV with visual correction.

Table 1 3.1-in. LF VR LCD specification.

3.1-in. LF VR LCD	
Resolution	3240 \times 2880
Pixel per inch	1411
MPRT	1.1 ms
FOV	100 deg \times 65 deg
Pixel per degree	15
Visual correction	Active



Fig. 15 Prototype demonstration.

4 Conclusion

Our paper presents a comprehensive exploration of a 3K3K, FOV 100-deg high-resolution LF display. We highlight the advancements in circuit and driver designs, propose pixel architectures to enhance image quality, showcase the benefits of LF technology in visual correction, and demonstrate the expansion of the eyebox using LF techniques. This work significantly contributes to the advancement of LF displays and lays the foundation for future developments in high-resolution VR systems with enhanced visual experiences.

Data Availability

Data underlying the results presented in this paper are not publicly available at this time but may be obtained from the authors upon reasonable request.

Acknowledgments

This research was partially supported by the Technology Development Programs from Ministry of Economic Affairs, Taiwan (Grant No. 108-EC-17-A-24-I1-0003).

References

1. B. C. Kress and W. J. Cummings, "11-1: invited paper: towards the ultimate mixed reality experience: HoloLens display architecture choices," *SID Symp. Digest of Tech. Pap.* **48**(1), 127–131 (2017).
2. J. Xiong et al., "Augmented reality and virtual reality displays: emerging technologies and future perspectives," *Light: Sci. Appl.* **10**(1), 216 (2021).
3. K. Yin et al., "Advanced liquid crystal devices for augmented reality and virtual reality displays: principles and applications," *Light: Sci. Appl.* **11**(1), 161 (2022).
4. E. L. Hsiang et al., "AR/VR light engines: perspectives and challenges," *Adv. Opt. Photonics* **14**(4), 783–861 (2022).
5. S. W. Min et al., "Three-dimensional electro-floating display system using an integral imaging method," *Opt. Express* **13**(12), 4358–4369 (2005).
6. X. B. Dong, L. Y. Ai, and E. S. Kim, "Integral imaging-based large-scale full-color 3D display of holographic data by using a commercial LCD panel," *Opt. Express* **24**(4), 3638–3651 (2016).
7. X. Sang et al., "Interactive floating full-parallax digital three-dimensional light-field display based on wavefront recomposing," *Opt. Express* **26**(7), 8883–8889 (2018).
8. H. Hua, "Enabling focus cues in head-mounted display," *Proc. IEEE* **105**(5), 805–824 (2017).
9. A. Wilson and H. Hua, "Design and demonstration of a varifocal optical see-through head mounted display using freeform Alvarez lenses," *Opt. Express* **27**(11), 15627–15637 (2019).
10. D. Dunn et al., "Towards varifocal augmented reality displays using deformable beam splitter membranes," *SID Symp. Digest Tech. Pap.* **49**(1), 92–95 (2018).
11. Y. Wu et al., "70-3: Invited paper: high-resolution light-field VR LCD," *SID Symp. Digest Tech. Pap.* **53**, 945–948 (2022).
12. G. Tan et al., "Foveated imaging for near-eye displays," *Opt. Express* **26**(19), 25076–25085 (2018).
13. F. Peng et al., "Analytical equation for the motion picture response time of display devices," *J. Appl. Phys.* **121**(2), 023108 (2017).
14. Z. Yang et al., "Reducing the power consumption of VR displays with a field sequential color LCD," *Appl. Sci.* **13**(4), 2635 (2023).

15. C. L. Yang et al., "High resolution HDR VR display using Mini-LED," *SID Symp. Digest Tech. Pap.* **52**(1), 636–639 (2021).
16. Y.-H. Wu et al., "Invited paper: high dynamic range 2117-PPI LCD for VR displays," *SID Symp. Digest Tech. Pap.* **54**, 36–39 (2023).
17. T. Zhou et al., "2117PPI VR LCD with ultra-high aperture opening ratio," *SID Symp. Digest Tech. Pap.* **54**, 1196–1199 (2023).
18. J. Y. Wu et al., "Image adaptation to human vision (eyeglasses free): full visual-corrected function in light-field near to eye displays," *SID Symp. Digest Tech. Pap.* **52**(1), 1143–1145 (2021).

Yung-Hsun Wu obtained his PhD in optics and photonics from the University of Central Florida. He is currently senior director of Innolux's technology development center, focusing on mobile and VR display advancements. Since 2017, his team has been dedicated to high-resolution VR research, notably introducing a VR LCD with 2000 PPI. His scholarly portfolio includes 50+ published papers on liquid crystal fast response devices and display applications.

Chuan-Chung Chang holds a PhD in optics and photonics from National Central University, Taiwan. His expertise includes optical inspection, systems, and computational imaging, with a role as senior director at Coretronic's Advanced Optical Technology Center, focusing on AR optical engine R&D. He has authored 45+ papers, holds 112 patents, is a member of Optica, SPIE, SID, and serves as director at Taiwan's 3DIDA.

Yu-Shih Tsou holds a PhD in optoelectronics from National Chiao Tung University, Taiwan. He currently oversees the optics design team at Innolux's technology development center, with a specific focus on optics within display technologies.

Yi-Chien Lo completed his PhD in optics and photonics at National Central University, Taiwan, in 2011. Subsequently, he engaged in postdoctoral research focused on illumination and imaging projects within the university's Department of Optics and Photonics from 2012 to 2015. Since 2017, he has held the position of principal engineer for AR/VR projects at Coretronic Corp. in Taiwan.

Chia-Hao Tsai achieved a master's degree in mechanical engineering from the Graduate Institute of Opto-Mechatronics at the National Chung Cheng University, Taiwan. At present, he is the director of the design team at Innolux's technology development center, with a dedicated emphasis on advancements in mobile and VR display technologies.

Chih-Hung Lu brings a profound understanding of image processing, computer vision, and three-dimensional optical measurement. He obtained a master's degree in communication engineering from National Central University, Taiwan. Throughout his tenure at Coretronic, he has honed his skills through practical involvement in projects spanning near-eye light field display, HUD, and CGH.

Chiu-Lien Yang completed her PhD in optoelectronics at National Chiao Tung University, Taiwan. She presently holds the esteemed position of chief technology officer at Innolux.

Fu-Ming Chuang earned his PhD from the Optical-Electronic Science Institute at National Central University, Taiwan. His extensive optics experience encompasses lenses for cameras, projections, microscopy, spectrometers, CCM lenses, interferometers, and more. He is an authority in domains like microstructure optics, LCD backlighting, stereo displays, and automotive optics. Notably, he has held significant roles, including CTO at Coretronic, vice president at 3DIDA Taiwan, and a SID Taipei Chapter board member.